Improve Risk Management and Decision-Making for Catastrophic Event Insurance using Return Level Estimation for Spatial Extremes

Sam Jun[1] and Bo Li[2]

Abstract

Insurance company relies on the estimation of extreme events when handling catastrophic event insurance. We introduce a newly developed method of estimating return levels of spatial extremes by taking spatial heterogeneity and smoothness into account. We expect the new method can help improve the risk management and facilitate better decision-making for catastrophic event insurance.

Keywords: Catastrophe, exceedance probability, event loss table, probable maximum loss, Spatial extremes

1. Introduction

Over the past few decades, catastrophe modeling has evolved as an essential component in risk management and decision-making process in the property insurance industry. A robust estimation of tail losses is particularly important for reinsurers due to the highly skewed and correlated nature of claims arising from natural catastrophe events, which significantly increases the magnitude of loss for high return periods. Thus, it is crucial for property (re)insurance companies to have a model that can generate a full probabilistic distribution of catastrophe losses in order to better understand and manage their exposure to natural hazards within their portfolio.

Since the claims due to natural catastrophe events are geographically correlated and occur infrequently compared to other perils such as automobile accidents or liability, the traditional actuarial models that utilize past loss experience to estimate future losses can significantly underestimate the risk. For instance, the 2011 Thailand Floods is considered to be the worst flooding event in at least five decades, with an estimated economic loss of more than 46 billion USD. This unprecedented event revealed that the pricing of flood risk in Thailand has previously

[1] [2]Department of Statistics, University of Illinois Urbana-Champaign

been inadequate, leading to major revisions in policy coverages and premiums. Thus, it is necessary to extrapolate the historical records to account for potential extreme events that may not yet have been recorded but are likely to happen in the future of a given time frame (e.g., 1-in-100 years, 1-in-200 years). This can be achieved through either physical model simulations or extreme value analysis using statistical models.

The exceedance probability (EP) curve, a loss curve representing the probability that the annual occurrence or aggregate loss exceeds various levels of loss, is a standard way of expressing the outputs of a catastrophe model. The occurrence exceedance probability curve (OEP) is the distribution of the largest event loss in a year, and the aggregate exceedance probability curve (AEP) is the distribution of the sum of all event losses in a year. EP curves can also be expressed in terms of return periods instead of exceedance probabilities, which are simply the inverses of each other. For instance, if the probability of experiencing an annual loss greater than $X is 1%, then $X can be expected to be exceeded once every 100 years. In general, the loss associated with exceedance probability of p is said to be the return level or probable maximum loss (PML) associated with $1/p$ year return period. An example of a OEP and AEP curve is shown in Figure 1. Note that AEP always has a higher PML than OEP for a given return period.

The EP curves are standardly obtained from commercial catastrophe models that can be licensed from model vendors (e.g., RMS and Verisk). Additionally, insurance companies may choose to develop their own models and/or return period estimates to incorporate any potential non-modelled risks that are not explicitly covered by readily available vendor models on the market.

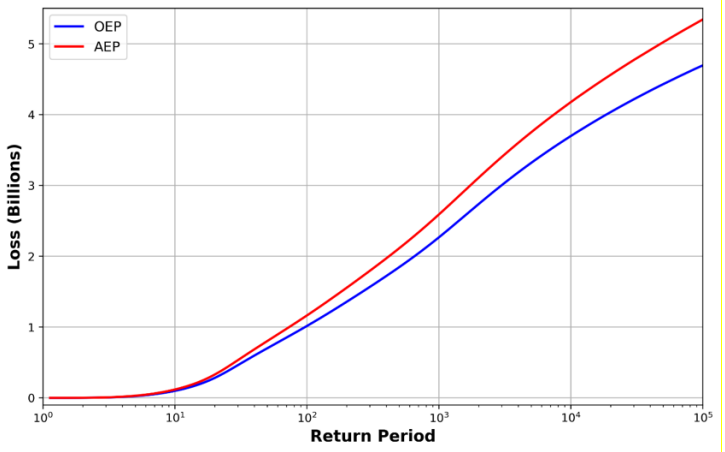

Figure 1: Example of a OEP and AEP curve

1.1 Uses of EP Curves in Insurance

The EP curves are used for wide array of business activities in (re)insurance industry such as underwriting, pricing, and portfolio management. For instance, an insurance company can calculate the probability of experiencing an annual loss that would exceed its survival constraint and determine how much reserve they need to hold in order to keep the likelihood of insolvency at an acceptable level based on the company's risk appetite. Alternatively, the company may raise premium, increase deductible, or purchase catastrophe bonds or reinsurance to shift the EP curve so that the probability that the annual loss exceeds the insurer's surplus is below a certain level. Similarly, the decision to underwrite a new policy can be made by analyzing the impact of adding the policy to the portfolio on the EP curve and the return period values.

Another important use of EP curve is in catastrophe ratemaking and reinsurance pricing. An insurance premium is the price that the insurer should charge the policyholders to cover losses, expenses, and generate profit for the company. For catastrophe ratemaking, there is an additional component called a risk load to reflect the extra cost of capital associated with the highly volatile nature of catastrophe losses. An insurance rate is defined as the average premium per exposure unit and can be calculated as

$$\begin{aligned} Rate &= \frac{Premium}{Exposure} \\ &= \frac{Loss + Expense + Risk\ Load + \ UW\ profit}{Exposure} \\ &= \frac{Pure\ Premium + Risk\ Load\ Per\ Exposure + \ Fixed\ Expense\ Per\ Exposure}{1 - Variable\ Expense\ Ratio - Profit\ Ratio}. \end{aligned}$$

The pure premium, or loss cost, is the expected cost of covering losses from claims and is typically derived by trending historical loss cost for traditional perils. This component is typically replaced by or blended with the expected loss from the EP curve for catastrophe perils. For calculating the risk load, a commonly used technique is a method developed by Kreps, which expresses the risk load as the expected return on the amount of surplus required to cover the loss at a desired return period, as shown in the formula below.

$$Risk\ Load = y * S = y * (Z * \sigma - Risk\ load).$$

Therefore, we have

$$Risk\ Load = \left(\frac{y * Z}{1 + y}\right) * \sigma,$$

where y is the expected yield rate, S is the required surplus, σ is the standard deviation of the loss from the EP curve, and Z is the distribution percentage point corresponding to the acceptable exceedance probability.

1.2 Catastrophe Models

A catastrophe model typically consists of three major components: hazard module, vulnerability module, and financial module. When the exposure data containing information about insured properties and their location are input to the catastrophe model, the hazard module outputs the local intensity of potential future catastrophe events at each site of interest. In a probabilistic model, these events are developed by combining historical data with physical, theoretical, and statistical models and are each assigned a rate of occurrence and a hazard footprint to represent the full range of possible event scenarios that could happen in the future.

As an illustration, an event set for river flooding may be developed as follows: First, a flood frequency analysis can be done by modeling the probability distribution of annual maxima discharge from instrumental river flow or rainfall data using extreme value theory. The spatial dependency can be captured by modeling the joint distribution of river flows at multiple sites using multivariate extreme value models such as copula models (Jongman et al., 2014) or conditional models (Heffernan and Tawn, 2004). The flow rate can be linked to a flood intensity measure (e.g., water depth) through hydrological and hydraulic modeling, which can be used to create a flood hazard map for specified return periods. Next, a synthetic set of flood events, defined in terms of the maximum river flow caused by a precipitation event, can be generated from a stochastic weather generator or a multivariate statistical model (Schneeberger and Steinberger, 2018). Then, an event footprint can be obtained for each event by finding the return period of river flow experienced at each site and interpolating the flood severity measure from the hazard maps created in the first part.

For instance, suppose that a hypothetical precipitation event leads to a flow rate of 1200 m^3/s at location x, which corresponds to a return period of 150 years (RP 150) according to the frequency analysis of annual maxima discharge. Suppose that we have hazard maps of flood depth corresponding to RP 100 and RP 200 river flow. Then, we can interpolate between the values of RP 100 and RP 200 hazard maps to find the flood depth corresponding to RP 150 at location x. This process can be repeated for all locations impacted by the event to create complete hazard footprints for all events in the event set. An alternative approach is a direct simulation of the precipitation events and their footprints by physical modeling, which remains computationally challenging to this date.

Using the event footprints from the hazard module, the vulnerability module translates the intensity of the hazard into physical damage of the insured properties along the event footprint by modeling the damageability of the properties based on the building characteristics provided in the exposure data, which includes information such as their location, number of floors, structure type, and building material. The degree of physical damage to a building is expressed as a mean damage ratio (MDR), where 0% implies no loss and 100% implies a total loss of the property. The mean damage ratio is multiplied to the total insured value (TIV) to convert property damage to financial loss.

After the loss at the location level are determined for each event by the vulnerability module, the financial module calculates the loss due to each event by applying the individual policy terms and aggregates them over all locations. The output of the financial module is an event loss table (ELT) for the entire portfolio, which can be used to obtain the EP curve discussed in the previous section.

1.3 Generating EP Curve from ELT

There are two main types of uncertainties in a catastrophe model that need to be considered when calculating the loss distribution from the ELT: primary and secondary. The primary uncertainty is the uncertainty about location, size, and frequency of future catastrophe events and is captured by the stochastic event generation process in the hazard model. The secondary uncertainty refers to the uncertainty in the loss estimate and comes from the estimation of intensity and damage in the hazard and vulnerability module, respectively. The secondary uncertainty can be quantified

as a distribution of damage ratio around the mean damage ratio, which is propagated through the loss calculation steps in the financial module to yield the standard deviation of the loss.

Table 1 provides an example of an event loss table. An event loss table includes an Event ID, the rate of the event, the average loss for the event given that it occurs, independent and correlated standard deviations of the loss, and the total amount of limits exposed. The primary uncertainty is reflected by rate and mean loss parameters, and the secondary uncertainty is represented by the standard deviation parameters. The standard deviation is split into independent and correlated components to address the dependency of the loss between the properties when aggregating the losses for a multi-location portfolio, where complete correlation implies a perfect linear relationship in the degree of damage between two locations and complete independence implies that the degree of damage in one location is completely unrelated to the other. For instance, the dispersion of loss impact for certain perils and regions may be more widespread and diffuse than others, which will result in a lower weight for the correlated component of the standard deviation. Also, a portfolio with higher density of exposures will be given a higher weight for the correlated standard deviation to reflect the fact that two losses will be more correlated if the distance between their locations is smaller.

OEP curve can be calculated directly from the ELT if the Poisson distribution is assumed for the annual frequency of events. For AEP calculation, a standard practice is to simulate the frequency and severity of the events using the parameters from the ELT to obtain a year-event loss table (YELT), a table of simulated loss by year and event. Table 2 provides an example. After applying the appropriate policy terms to each event occurrence in the YELT, the net losses can be aggregated for all events in a year to yield a year-loss table (YLT), which can easily be converted to an AEP curve. A common choice of probability distribution for simulating the number of events is Poisson distribution, and the severity of the event is typically generated by simulating a damage ratio from Beta distribution and multiplying it to the total amount of limits exposed.

Table 1: Sample ELT

Event ID	Rate	Mean Loss	Sdi	Sdc	Exposure
1	0.10	500	500	500	10,000
2	0.10	300	400	800	5,000
3	0.50	200	300	400	4,000

Table 2: Sample YELT

Year	Event ID	Loss
1	41	10,000
3	2	300
3	35	10,000
…	…	…
10,000	2	5,000

2. Return level estimation for spatial extremes

Return level corresponding to a particular return period, also called probable maximum loss (PML), plays a central role in the hazard and the subsequent modules. Since natural hazards are often observed in a spatial domain, we proposed a flexible and fast method to estimate spatial return levels based on extreme value distribution (Sass et al., 2021). Our method can provide accurate return level estimates and meantime improve both the primary and secondary uncertainty quantification by considering the heterogeneity and smoothness of spatial return levels.

The first thing to apply extreme value theory is to identify extreme values. Classifying extreme values is commonly done in two ways: block maxima and peaks over threshold. The block maxima approach divides the dataset into equal periods and chooses the maximum value from each period. The generalized extreme value (GEV) distribution is the limiting distribution of block maxima and is known to fit accurately for large blocks (Fisher and Tippett 1928; Gumbel 1958; Coles 2001). The block maxima approach can be wasteful as it only chooses one point from each period. In the peaks over threshold approach, a threshold limit is chosen and all points

exceeding the limit are selected to form the extreme dataset. For a high enough threshold, the generalized Pareto distribution (GPD) arises as the limiting distribution to model data over the threshold (Pickands 1975; Davison and Smith 1990).

Many techniques for modeling spatial extreme data have been developed for modeling the site-wise marginal behavior that is highly related to return level. Characterizing the marginal distribution is often done through latent variable models (Coles and Casson 1998; Casson and Coles 1999; Cooley, Nychka, and Naveau 2007; Sang and Gelfand 2009). Latent variable models introduce spatial variation through Gaussian processes of the parameters of the marginal distribution. This is often accomplished via a hierarchical specification of the joint distribution followed by Bayesian inference which is computationally intensive and dependent on prior distributions. Besides latent variable models, the spatial GEV and spatial GPD are perhaps the simplest and fastest approach to modeling the spatial variation of marginal distributions. These methods assume marginal independence and only account for dependence by allowing the parameters to vary spatially through linear functions.

2.1 Fused Spatial GEV and GPD Models

Due to their computational efficiency, the spatial GEV and spatial GPD can be applied to large spatial extremes data. Surprisingly, the return level estimation based on spatial GEV is shown to be comparable to various max-stable models (Cao and Li 2018). However, if the spatial domain of observations is vast, the constant shape parameter usually assumed in the spatial GEV and GPD will likely be violated and this may cause deteriorated return level estimation as return levels are very sensitive to even a small perturbation of the shape parameter. Furthermore, the location and scale parameters in those two models may not simply follow a parametric relationship with the available covariates. In such cases, it would be more appropriate to account for the spatial heterogeneity of the shape parameter, as well as to allow for flexible forms of spatial variability in location and scale parameters. Assume the marginal distribution of extremes is GEV with location, scale and shape parameter. We assume all three parameter are spatially varying, i.e, they can be denoted as $\mu(s)$, $\sigma(s)$ and $\xi(s)$.

Unlike Bayesian methods that assume a latent Gaussian process for the parameters, we propose to regulate the shape parameter using the fused lasso or fused ridge penalty. To attain flexibility of other parameters that are usually restricted to a parametric, often linear, form in the spatial GEV and spatial GPD, we further propose to regulate all three parameters in the spatial GEV or two parameters in the spatial GPD using a fused lasso or fused ridge penalty. The fused penalty has been used to model the clustering pattern or smoothness of spatial data by penalizing differences in parameter estimations of nearby locations (Tibshirani and Taylor 2011; Parker, et al. 2016; Tansey et al. 2018; Li and Sang 2019).

Our fused spatial extremes models share the advantage of the traditional spatial GEV and GPD models for being applicable to large data sets, however, our models allow for a nonparametric representation when describing the spatial variability of the GEV and GPD parameters and thus largely improves the return level estimation. Compared to max-stable models that demand a dependency structure, our fused spatial extremes models do not require such specifications but rather regulates spatial variability through the penalties. Compared to Bayesian implementation of max-stable models that are usually computationally intensive for handling large covariance matrices, our methods dramatically improve the computational efficiency. Furthermore, the proposed models require no stationarity assumption which is commonly made in modeling spatial extremes.

The theory and exposition of the spatial GEV and GPD models with fused penalties can be found in Sass et al. (2021). A block bootstrap was used to derive the uncertainty of the return level estimates. To demonstrate the method, we show its application to spatial weather extremes.

2.2 Return Level Estimation for Precipitation Data

We analyzed climate model output on annual maximum daily precipitation over historical (1969–2000) and future conditions (2039–2070) for 2622 sites across the continental United States. These data were provided by the North American Regional Climate Change Assessment Program (NARCCAP) and can be downloaded from the website http://www.narccap.ucar.edu/index.html. The NARCCAP chose the A2 emissions scenario, which is described in Nakicenvoic et al. (2000). The output data were produced using the Geophysical Fluid Dynamics

Laboratory's AM2.1 climate model with 50km resolution. NARCCAP provides eight 3-hr precipitation rates each day, and we compute the daily total by summing these eight values and multiplying by three. We then analyze the annual maximum of the daily precipitation totals from the two time-slices separately using the fused spatial GEV model under either ridge or lasso penalty.

The nature of the fused penalty in our fused spatial GEV restricts the parameter estimates and thus the return level estimates to only site- wise locations. In order to estimate the return level at unknown locations, we interpolated using ordinary kriging. Kriging is a traditional approach for spatial data interpolation that exploits the spatial correlation between observations. Cao and Li (2018) showed that kriging interpolated return levels performed qualitatively similar as the return level estimation based on max- stable models when data follow a max-stable model.

Given the long time period considered, it is unlikely that the data is stationary across time. To account for the non- stationarity, we incorporate a simple linear time trend into the location parameter. We model $\mu(s, t) = \alpha(s) + \beta(s)t$, where $\alpha(s)$ is the spatially varying location parameter, $\beta(s)$ is the spatially varying coefficient associated with the time trend, and t=1for years 1969 and 2039,up to t=32 for years 2000 and 2070.

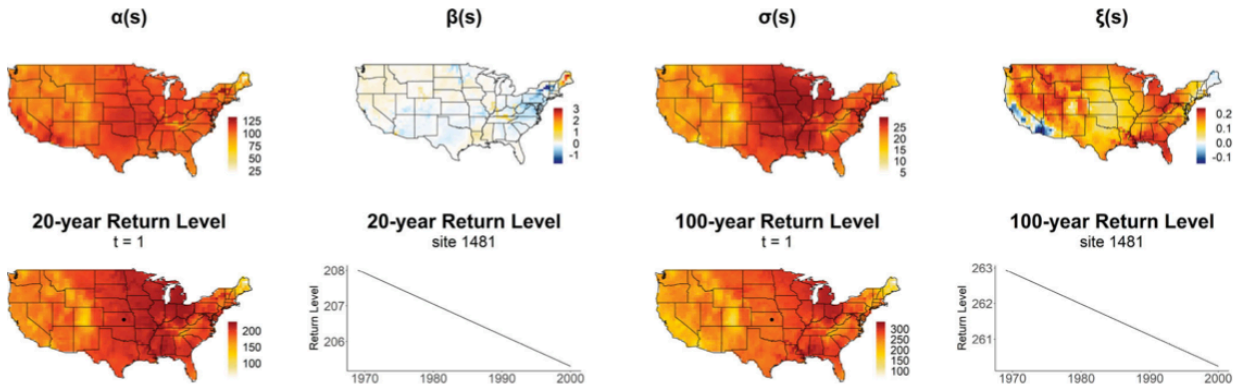

Figure 2 . Estimated GEV parameters, 20-, and100-year return level for the historical simulation using the fused ridge model. The spatially varying return levels are shown at time t=1 (year 1969) and the time varying return levels are shown for site 1481, located at the black dot. All units are mm/h.

Figure 2 shows the estimated GEV parameters, 20-, and 100-year return level for the historical simulation using the fused ridge model. Since we model the location parameter as a function of

time, the return level is also a function of time. For illustration purposes, we plot the 20- and 100-year return level map at time, t = 1, and the time varying return level for a single site, s = 1481. The results for the fused lasso model are very close to those of the fused ridge so we omit the fused lasso plots. The estimated location and scale parameters are highest in the midwest. There is a positive trend in the northwest and the largest negative trend is in Virginia. The generally positive shape parameter indicates a heavy tailed distribution with no upper bound. The 20-year return level tends to mimic the high and low estimates of the location and scale parameters. The 100-year return level shows an increased precipitation in Ohio and Kentucky heavily influenced by the larger shape parameter. However, the negative trend in Ohio and Kentucky suggests the return level will decrease when estimated at a later time, for example at t = 32.

2.3 Annual Maximum Temperature Change

To demonstrate the ability of the fused models to handle even larger datasets, we analyze annual maximum temperature data for 8,125 sites across the continental US for the years 1898–1997. The data were provided by the National Corporation for Atmospheric Research (NCAR) and is available upon request from Dr. Douglas Nychka. Observed data at each station was used when available and any missing station values were filled in using spatial statistics to produce a complete dataset (Johns et al. 2003). A more detailed description of the data can be found at https://www.image.ucar.edu/Data/US.monthly.met/. We split the data into two equal time periods of 50 years and estimate the return levels for each time period separately.

Given the long time period, we model the location parameter as in precipitation data to account for nonstationarity, where t = 1 represents years 1898 and 1948, up to t = 50 for years 1947 and 1997.

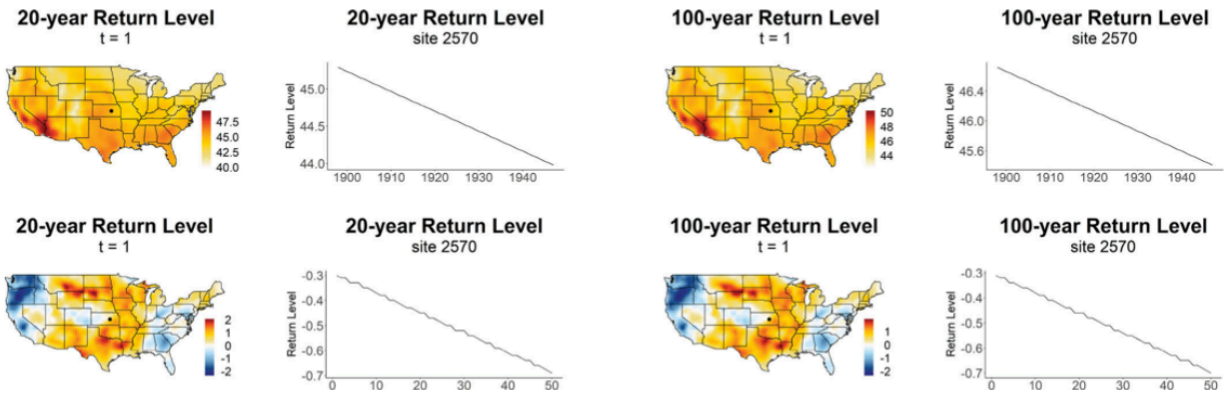

Figure 3. Top: estimated 20- and 100- year return level for the years 1898–1947 using the fused ridge model. Bottom: estimated change in 20- and 100-year return level between the years 1898–1947 and 1948–1997 using the fused ridge model. The spatially varying return levels are shown at time t = 1 (1898 and 1948) and the time varying return levels are shown for site 2570, located at the black dot. All units are in degrees Celsius.

The return level estimates in the top row of Figure 3 suggest the hottest maxima temperatures are in the southwest while the lowest maxima temperatures are along the rocky mountains in Colorado and Wyoming. Lower return levels are also expected in the northeast and along the Washington coastline. This follows the intuition of what one generally expects when thinking of historical temperatures across the United States.

It is known that average temperatures in the United States since 1900 have warmed on average, however it is less clear whether maximum temperatures have changed during this period (Lee, Li, and Lund 2014). The bottom row of Figure 3 shows the change in return level estimates between the two time periods at time t=1, 1898 and 1948. From the plots we can see the temperature has the largest increases in the midwest. At time t = 1, 3,178 of the 8125 stations had a decrease in annual maximum temperature for the 100-year return level. Compared to time t = 50, 6264 of the 8125 stations had a decrease in annual maximum temperature.

3. Discussion

Accurate return level estimates of spatial extremes can improve risk management and better facilitate decision-making for catastrophic event insurance. We developed fused spatial GEV and fused spatial GPD models with varying coefficients under either a ridge or lasso penalty in our recent paper, Sass et al. (2021). Our proposed models are flexible in parameterization and thus

are able to capture the spatial variability of the data better than the spatial GEV and spatial GPD with parametric parameter specifications. Our models require no assumption of stationarity and are significantly more computationally efficient compared to Bayesian models. The simulation study showed that the proposed models outperform spatial GEV, spatial GPD, and max-stable models when the marginal GEV and GPD vary spatially. Our models also outperform Bayesian models when the spatial extremes process is smooth or when the spatial extremes data show nonstationary dependence. While in general Bayesian models yield the most accurate return level estimation, their extensive computation may discourage users. The fused spatial models with ridge penalty are obviously suitable for smoothly varying marginal behavior, while if the marginal GEV or GPD distribution of the spatial extremes is spatially clustered, then the fused lasso models are expected to be more appropriate.

We used precipitation and temperature to demonstrate the ability of the fused spatial extremes models to produce practical return level maps for large datasets, but the method can be easily extended to the annual maximum discharge or other types of extremes in the hazard module. We expect our new method will help insurance industry more precisely manage the catastrophic event insurance.

References

Cao, Y., & Li, B. (2018), Assessing Models for Spatial Extremes and Methods for Uncertainty Quantification on Return Level Estimation, *Environmetrics*, 30, 1-21.

Casson, E., & Coles, S. (1999), Spatial Regression Models for Extremes, *Extremes*, 1, 449–468.

Coles, S. (2001), *An Introduction to Statistical Modeling of Extreme Values*, London, UK: Springer-Verlag London.

Coles, S., & Casson, E. (1998), Extreme Value Modelling of Hurricane Wind Speeds, *Structural Safety*, 20, 283–296.

Cooley, D., Nychka, D., & Naveau, P. (2007), Bayesian Spatial Modeling of Extreme Precipitation Return Levels, *Journal of the American Statistical Association*, 102, 824–840.

Davis, G., Gotham, S., Frith, A., Christie, J, Caravaggio, S. (2018). Incorporation of Flood and Other Catastrophe Model Results into Pricing and Underwriting.

Davison, A. C., & Smith, R. L. (1990), Models for Exceedances Over High Thresholds, *Journal of the Royal Statistical Society, Series B*, 52, 393-442.

Fisher, R. A., & Tippett, L. H. C. (1928), On the Estimation of the Frequency Distributions of the Largest or Smallest Member of a Sample, *Proceedings of the Cambridge Philosophical Society*, 24, 180-190.

Gumbel, E. J. (1958), *Statistics of Extremes*, New York: Columbia University Press.

Heffernan, J. E., & Tawn, J. A. (2004). A conditional approach for multivariate extreme values (with discussion). *Journal of the Royal Statistical Society: Series B (Statistical Methodology)*, *66*(3), 497-546.

Homer, D., & Li, M. (2017, June). Notes on using property catastrophe model results. In *Casualty Actuarial Society E-Forum* (Vol. 2, pp. 1-15).

Johns, C., Nychka, D., Kittel, T., & Daly, C. (2003), Infilling Sparse Records of Spatial Fields, *Journal of the American Statistical Association*, 98, 796–806.

Jongman, B., Hochrainer-Stigler, S., Feyen, L., Aerts, J.C., Mechler, R., Botzen, W.J., Bouwer, L.M., Pflug, G.C., Rojas, R., & Ward, P.J. (2014). Increasing stress on disaster-risk finance due to large floods. Nature Climate Change, 4, 264-268.

Kreps, R. (1990). Reinsurer risk loads from marginal surplus requirements. In Proceedings of the Casualty Actuarial Society (Vol. 77, pp. 196-203).

Lee, J., Li, S., & Lund, R. (2014), Trends in Extreme U.S. Temperatures, *Journal of Climate*, 27, 4209–4225.

Li, F., & Sang, H. (2019), Spatial Homogeneity Pursuit of Regression Coefficients for Large Datasets, *Journal of the American Statistical Association*, 114, 1050–1062.

Mitchell-Wallace, K. (2017). *Natural catastrophe risk management and modelling: A practitioner's guide*. John Wiley and Sons, Inc.

Nakicenovic, N., Alcamo, J., Davis, G., & De Vries, B. (2000), Special Report on Emissions Scenarios: A Special Report of Working Group III of the Intergovernmental Panel on Climate Change. Cambridge: Cambridge University Press.

Parker, R. J., Reich, B. J., & Eidsvik, J. (2016), A Fused Lasso Approach to Nonstationary Spatial Covariance Estimation, *Journal of Agricultural, Biological, and Environmental Statistics*, 21, 569–587.

Pickands, J. (1975), Statistical Inference Using Extreme Order Statistics, *Annals of Statistics*, 3, 119–131.

Sass, D., Li, B. & Reich, B.J. (2021). Flexible and fast spatial return level estimation via a spatially fused penalty. *Journal of Computational and Graphical Statistics*, 30(4), 1124-1142.

Sang, H., & Gelfand, A. E. (2009), Hierarchical Modeling for Extreme Values Observed Over Space and Time, *Environmental and Ecological Statistics*, 16, 407–426.

Schneeberger, K., & Steinberger, T. (2018). Generation of spatially heterogeneous flood events in an alpine region—Adaptation and application of a multivariate modelling procedure. *Hydrology*, *5*(1), 5.

Tansey, W., Koyejo, R. P., & Scott, J. (2018), False Discovery Rate Smoothing, *Journal of the American Statistical Association*, 113, 1156– 1171.

Tibshirani, R. J., & Taylor, J. (2011), The Solution Path of the Generalized Lasso, *Annals of Statistics*, 39, 1335–1371.